Journal of Catalysis **201,** 46–59 (2001)
doi:10.1006/jcat.2001.3232, available online at http://www.idealibrary.com on IDEAL®

Photocatalytic Degradation of Dyes in Water: Case Study of Indigo and of Indigo Carmine

Manon Vautier, Chantal Guillard, and Jean-Marie Herrmann[1]

Laboratoire de Photocatalyse, Catalyse et Environnement LPCE (IFoS UMR CNRS n°5621), Ecole Centrale de Lyon, B.P. 163, 69131 Ecully cedex, France

Received October 24, 2000; revised March 13, 2001; accepted March 23, 2001; published online May 31, 2001

The TiO_2/UV photocatalytic degradations of indigo and of indigo carmine have been investigated both in aqueous heterogeneous suspensions and in the solid state. In addition to prompt removal of the color, TiO_2/UV-based photocatalysis was simultaneously able to oxidize the dye, with almost complete mineralization of carbon and of nitrogen and sulfur heteroatoms into CO_2, NH_4^+, NO_3^-, and SO_4^{2-}, respectively. A detailed degradation pathway has been determined by careful identification of intermediate products, in particular, carboxylic acids, whose decarboxylation by photo-Kolbe reactions constitutes the main source of CO_2 evolution. The only persistent organic compound was acetic acid, whose degradation required a longer period of time. These results suggest that TiO_2/UV photocatalysis may be envisaged as a method for treatment of diluted wastewaters in textile industries. The irradiation of titania with visible light did produce a photoinduced decolorization of the dye, probably induced by the breaking of the double-bond conjugation system of the chromophoric group. However, this decolorization was not accompanied by any degradation of the molecule since no loss of total organic carbon (TOC) nor release of inorganic ions were observed. This corresponded to a stoichiometric reaction of an electron transfer from the dye molecule excited in visible irradiation to titania. Because indigo is very poorly soluble (≈2 ppm), it was tentatively degraded in its solid state, mixed with titania in a photocatalytic solid-solid-type reaction. Observation of the decolorization and of the degradation of solid indigo constitutes a surprising and encouraging result for the development of self-cleaning titania-coated objects (glasses, steel, aluminium, metals, walls, etc.) fouled by solid dirt particles.

Key Words: **titania; photocatalysis; photocatalytic degradation; dyes; indigo; indigo carmine; water decolorization; water purification; solid indigo.**

INTRODUCTION

Fifteen percent of the total world production of dyes is lost during the dyeing process and is released in the textile effluents (1). The release of those colored wastewaters in the ecosystem is a dramatic source of esthetic pollution, eutrophication, and perturbations in aquatic life. As international environmental standards are becoming more stringent (ISO 14001, October 1996), technological systems for the removal of organic pollutants, such as dyes, have been recently developed. Physical methods, (adsorption (2)), biological methods (biodegradation (3, 4)), and chemical methods (chlorination and ozonation (5)) are the most frequently used.

Among the new oxidation methods or "advanced oxidation processes" (AOP), heterogeneous photocatalysis appears as an emerging destructive technology leading to the total mineralization of many organic pollutants (6–12), following the proposed mechanism:

—absorption of efficient photons ($h\nu \geq E_G = 3.2$ eV) by titania

$$(TiO_2) + h\nu \rightarrow e^-_{CB} + h^+_{VB}; \quad [1]$$

—oxygen ionosorption

$$(O_2)_{ads} + e^-_{CB} \rightarrow O_2^{\circ -}; \quad [2]$$

—neutralization of OH^- groups into $OH^\bullet$ by photoholes

$$(H_2O \Leftrightarrow H^+ + OH^-)_{ads} + h^+_{VB} \rightarrow H^+ + OH^\bullet; \quad [3]$$

—oxidation of the organic reactant via successive attacks by $OH^\bullet$ radicals

$$R + OH^\bullet \rightarrow R'^{\circ} + H_2O; \quad [4]$$

—or by direct reaction with holes

$$R + h^+ \rightarrow R^{+\circ} \rightarrow \text{degradation products.} \quad [5]$$

As an example of the last process, holes can react directly with carboxylic acids, generating CO_2 according to the so-called photo-Kolbe reaction:

$$RCOO^- + h^+ \rightarrow R^\circ + CO_2. \quad [6]$$

A general list of various families of organic pollutants that can be treated by photocatalysis has been given (13).

[1] To whom correspondence should be addressed. Fax: (33) 4 78 33 03 37. E-mail: jean-marie.herrmann@ec-lyon.fr.

0021-9517/01 $35.00

In most cases, the degradation is conducted for dissolved compounds in water with UV-illuminated titania. Possible limits of the technique concern the irradiation source and the physical state of the pollutant. Recently, some authors have reported the degradation of organic pollutants by visible light using photosensitization of the catalyst (14–17). The interest is to use solar light, which is free and inexhaustible. With respect to the physical state of the pollutant, very few studies have been devoted to the photocatalytic degradation of a solid. The only (undesirable) example concerns the chalking of pigmented coatings and plastics (18).

Indigo or 2,2′-bis-indole is not only one of the oldest dyes known but still is one of the most importantly used: It represents 3% of the total production of dyes. Its major industrial application is the dyeing of clothes (blue jeans) and other blue denim products (19). Its unusually high melting point (390–392°C) and its very poor solubility can be explained by the existence of strong intermolecular hydrogenbonds. In the solid state, indigo forms a polymer in which each indigo molecule is linked to four surrounding molecules. In nonpolar solvents, the indigo is present mainly as a monomer, whereas in polar solvents, intermolecular association occurs and the solutions are blue (1). The basic color-producing structure is a cross-conjugated system or H-chromophore, consisting of a single C=C double bond substituted by two NH donor groups and two CO acceptor groups (Scheme 1)

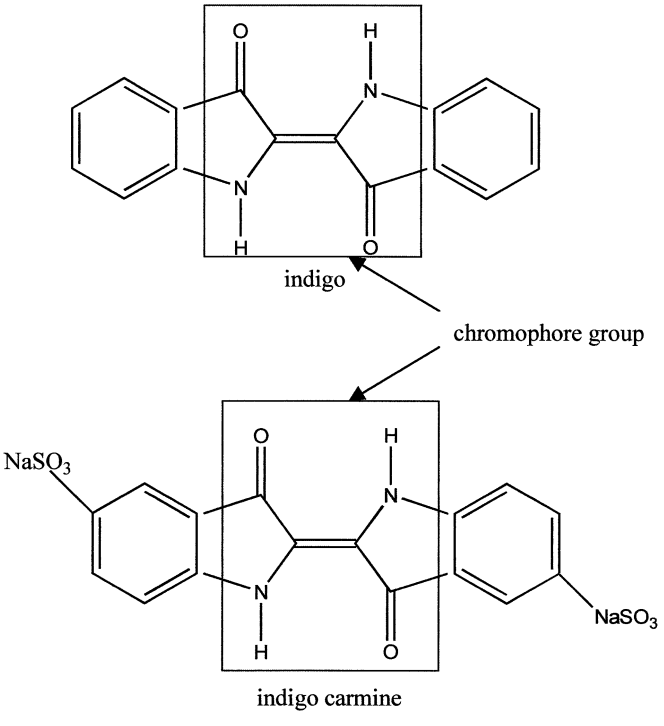

SCHEME 1. Developed formulae of indigo and of indigo carmine.

(20). Up to now, as far as we know, no studies have been devoted to the photocatalytic degradation of indigo (13) probably because of its too low solubility (21). In the present work, we studied the photocatalytic decolorization and degradation of indigo and of one indigoid dye, indigo carmine (indigo disulphonic-5,5′ acid (Scheme 1)), since its solubility in water enables one to perform a better kinetic study of degradation with easier identification of degradation intermediates. We studied successively (i) the photocatalytic degradation of indigo and of indigo carmine in water, (ii) the photoinduced decolorization of indigo carmine in water by irradiation of TiO_2 in visible irradiation, and (iii) the photocatalytic degradation of solid indigo.

EXPERIMENTAL

Materials

Indigo and indigo carmine were supplied by a textile firm and used as received. The photocatalyst was titania Degussa P-25 (anatase/rutile = 3.1; surface area = 50 m^2g^{-1}, nonporous particles). The slurry, which is not colloidal, consists of large fractal aggregates of individual particles, each one having a mean diameter, d, of ca. 30 nm, in agreement (i) with the value calculated from the formula (given as a function of the volumic mass ρ and the specific surface area S for homodispersed nonporous particles),

$$d = 6/\rho S,$$

and (ii) with transmission electron microscopy performed on sonicated samples.

Photoreactor and Light Source

Photocatalytic tests were performed in a batch microphotoreactor of 100 mL made of Pyrex (transmittance: $\lambda >$ 290 nm), which is described in Fig. 1. It was equipped with a high-pressure mercury lamp (Philips HPK 125 W). For visible irradiation, the same lamp was used but the light beams were filtered by a Corning 3-71 optical filter ($\lambda > 440$ nm) incorporated in the water cell used to remove IR beams from the lamp and to avoid heating. The UV irradiation enters the reactor through the bottom optical window made of Pyrex, which plays the role of a UV filter with transmittance for $\lambda \geq 290$ nm. The slurry is agitated with a magnetic stirrer whose magnet spins in a perpendicular plane. The temperature is maintained at 295 K using thermostated water in the jacket. The headspace of the photoreactor has three necks: one for liquid or slurry sampling through a septum; a central one with a vacuum-tight valve for gas sampling; and another one for possible introduction of products. In general, degradations were performed with the oxygen from the air since the kinetics, followed by analyses of the liquid phase, have indicated that atmospheric air in the headspace

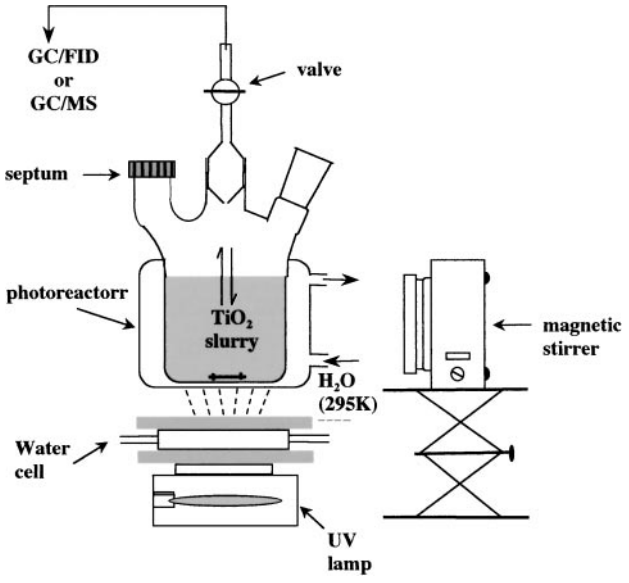

FIG. 1. Scheme of the slurry photoreactor used for photocatalytic dye degradation.

of the photoreactor provided enough oxygen for the oxidative degradation of pollutants. In these conditions, the necks were open to air.

Determination of the Efficient Photon Flux

The efficient photon flux was calculated from the radiant flux (in mW/cm^2) measured with a radiometer (United Detector Technology; model 21 A), calibrated against a microcalorimeter and by taking into account the lamp spectral distribution, the optical filter transmission, and the absorbance spectrum of titania, as commonly done in our previous studies.

Irradiation of the Slurry

The reactor was filled with 20 mL of an aqueous suspension of TiO_2 (50 mg, optimum concentration of catalyst, as in Ref. (22)) containing either indigo (total content: 200 ppm (i.e., 763 μmol L^{-1}), both dissolved (2 ppm) and mainly as a quasi-colloidal suspension) or indigo carmine (29 ppm or 64 μmol L^{-1}, totally dissolved). The initial corresponding pH's were equal to 4.6 and 4.8, respectively. Prior to illumination, the suspension was magnetically stirred in the dark for 30 min, corresponding to the time needed to establish the adsorption/desorption equilibrium at room temperature. During irradiation, stirring was maintained to keep the mixture in suspension. At regular intervals, samples of 0.5 mL were withdrawn for analysis. Before analyses they were centrifuged or filtered through 0.45-μm Millipore filter disks to separate TiO_2 particles.

Irradiation of the Solid Deposits

Two milliters of an aqueous suspension containing 0.79 g L^{-1} (3 mmol L^{-1}) indigo and 5.09 mg L^{-1} (64 mmol L^{-1}) TiO_2 were deposited on an optical disk made of Pyrex or on the inner bottom window of the photoreactor, which was closed for the gas phase analyses. Water was evaporated before irradiation.

Analyses

The decrease in the concentration of the dyes was observed from the characteristic absorption at $\lambda = 610$ nm for indigo carmine in water and at $\lambda = 710$ nm for indigo, using a UV–visible spectrophotometer (2000 Safas model). The adsorption of the dyes on the catalyst was characterized by a FT-IR spectrometer in attenuated total reflection (Perkin–Elmer).

The identification of reaction intermediates by HPLC and/or GC/MS required preconcentration because of the high dilution. For HPLC/UV detection of carboxylic acids, preconcentration was performed with an ion-exchange cartridge (SAX from Varian). It was activated with water buffered at pH 7. Some carboxylic acids were concentrated using the solid phase microextraction (SPME) technique with a 85-μm-thick polyacrylate film, commercialized by Supelco. For some acids, the fiber of the syringe was derivated with a solution of pyrenyldiazomethane (PDAM). The detection of aromatic compounds by GC/MS required preconcentration by liquid–liquid extraction: after acidification at pH 1 with H_2SO_4 and saturation by Na_2SO_4, extraction was performed three times with 20 mL of solution using 10 mL of diethyl ether, and the solution dried under vacuum and the resulting solid dissolved in 100 μL of *N*,*O*-bis(trimethylsilyl)trifluoroacetamid (BTFA) before injection in the GC/MS. The analyses of intermediate products were performed with a HPLC Sarasep column (length, 30 cm; inner diameter, 7.8 mm) equipped with a Waters 486 UV detector at 210 nm. The mobile phase was composed of H_2SO_4, 5×10^{-3} M and the flow rate was 0.7 mL min^{-1}. Some of the intermediate products were also identified by GC-MS, using a HP 5890 series II gas chromatograph (Chrompack CP-SIL 5-CB column; length, 25 m; inner diameter, 0.25 mm; film thickness, 1.2 μm), equipped with a HP 5971 mass selective detector operating in the electron impact mode. The injections were made in the splitless mode. The column program was 393–573 K (heating rate, 3 K min^{-1}; hold time, 5 min).

For the kinetics of gas products evolution, i.e., CO_2, the headspace was preliminarily filled with pure oxygen with all the necks closed. For gas sampling, the loop of the GC conductivity detector and the gas tubing connecting it to the valve of the photoreactor were evacuated and then maintained under static vacuum ($P \leq 10^{-2}$ Torr). The headspace gas volume was then expanded for a few seconds in the

evacuated loop of the CD chromatograph. The valve was closed and the gas contained in the loop was injected into the chromatograph by flushing the vacuum-tight six-way valve with the carrier gas. After injection, the loop and the tubing were evacuated until the next injection. The stainless steel tubing connecting the photoreactor to the loop had a small diameter of 1/16 in. to provide a total volume of (loop + tubing) limited to 2 mL. Since the headspace has a volume of 80 mL, this means that every sampling caused an expansion of 2.5%, i.e., a loss of 2.5% of gaseous products, which was taken into account for corrections. This procedure caused limited removal of gas for sampling without disturbance of kinetics determination. In addition, there was no contamination of the gas phase by the carrier gas. CO_2 was analyzed with an Intersmat IGC 120-MB gas chromatograph equipped with a Porapack Q column (length, 3 m; inner diameter, 1/4 in.), connected to a catharometer detector.

Mineralization into CO_2 was also determined in parallel by measurements of the total organic carbon (TOC) using a Shimadzu 5050-A TOC analyzer equipped with a SFM 5000 A solid sample module.

The formation of inorganic ions was detected with a Waters 431 electrical conductivity detector, equipped with a HPLC Waters IC-Pak Anion column (length, 50 mm; inner diameter, 4.6 mm) for the anions (mobile phase, borate gluconate; flow rate, 0.9 mL min^{-1}) and with a HPLC Vydac column (length, 300 mm; inner diameter, 7.8 mm) for the cations (mobile phase, HNO_3, 2.5×10^{-3} M; flow rate, 1.5 mL min^{-1}).

RESULTS AND DISCUSSION

1. Photocatalytic Degradation of Indigo and of Indigo Carmine in Water by TiO_2/UV

1.1. Real Photocatalytic Nature of the Reaction

To obtain relevant information about the photocatalytic degradation, it was necessary to carry out experiments from which any possible direct photolysis was excluded. Experiments were made (i) in the absence of TiO_2 (neat photochemical regime) and (ii) in the presence of UV-illuminated SiO_2 to detect any possible contact mass effect. In both cases, no disappearance of indigo carmine was observed. A complete disappearance of indigo carmine could only be observed with the simultaneous presence of titania and of UV light, as shown in Fig. 2. This indicates that the system is working in a pure photocatalytic regime.

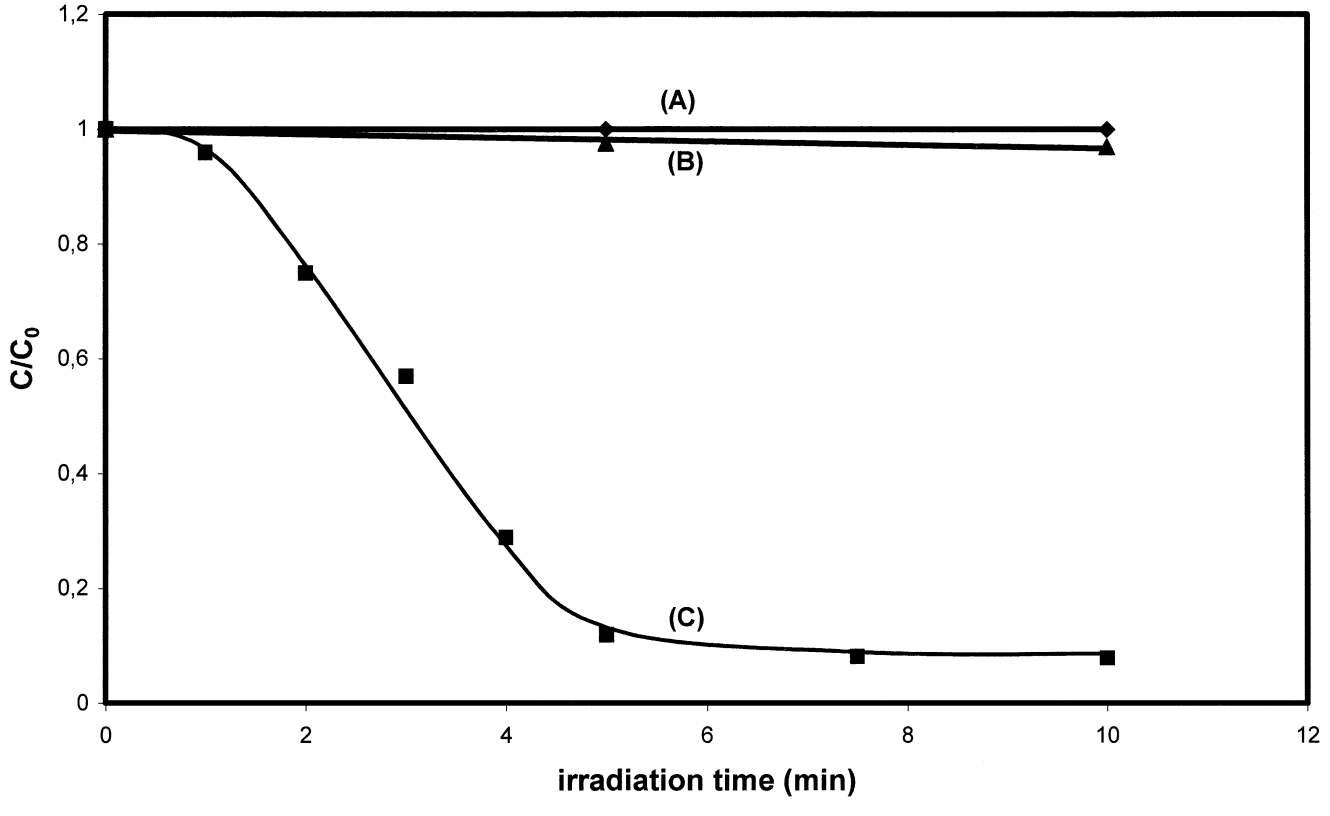

FIG. 2. Disappearance of indigo carmine ($C_0 = 61$ μmol L^{-1}). Curve A: UV irradiation ($\lambda \geq 290$ nm) alone. Curve B: UV irradiation with inert SiO_2. Curve C: UV irradiation with TiO_2.

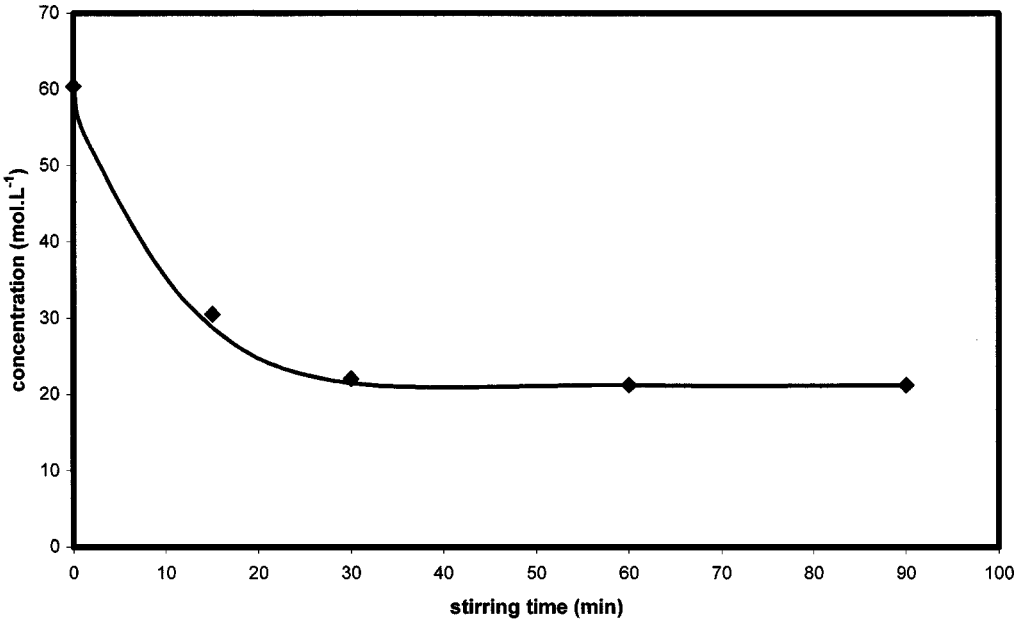

FIG. 3. Kinetics of adsorption of indigo carmine in the dark.

1.2. Adsorption of Indigo and of Indigo Carmine on TiO_2

The kinetics of adsorption in the dark is presented in Fig. 3. From the decrease in concentration of indigo carmine, the amount adsorbed was determined and corresponded to a surface coverage of 0.13 molecules nm^{-2}. In comparison with the maximum surface density of titania's OH groups (5 molecules nm^{-2} (23)), a relative surface coverage of ca. 3% can be estimated.

FT-IR investigations have been performed on each dye in the presence and in the absence of the photocatalyst. The results are the following: the modification of the asymmetric stretching vibrations of benzenesulfonic acids at 1081 and 1103 cm^{-1} caused by the absence or the presence of TiO_2 in indigo carmine indicates that the adsorption involved one of the sulfonate groups of the dye (Fig. 4, top). Adsorption through sulfonate groups has already been observed in the case of dye alizarin red (17). Because of the extreme positions of the sulfonate groups, the flat indigo carmine molecule may be considered as adsorbed perpendicularly to the surface of titania or at least obliquely, depending on its environment in the adsorbed layer. By contrast, for indigo, the shifts of the aromatic stretching vibration (1609 cm^{-1}) and of the intense skeletal bands at 1172, 1125, and 1063 cm^{-1} (Fig. 4, bottom) shows that indigo adsorption on TiO_2 mainly involves interactions with the aromatic rings. It would imply that indigo molecules adsorb parallel to the surface of TiO_2.

The amounts of in indigo carmine adsorbed on various solids has been correlated to their point of zero charge (PZC): PZC = 1.8, 9.1, and 6.7 for SiO_2, Al_2O_3, and TiO_2, respectively. The dye was completely adsorbed on alumina, partially on titania, and absolutely not on SiO_2. This reveals that the adsorption requires electrostatic interactions between the dye molecule and the hydroxyl groups of the photocatalyst.

Therefore, the difference in the adsorption mode between indigo and indigo carmine may produce some changes in the kinetics and in the mechanism of degradation (see next paragraphs).

1.3. Photocatalytic Degradation of Indigo Carmine and of Indigo

1.3.1. Kinetics of disappearance. The kinetics of disappearance of indigo carmine is represented in Fig. 2, with a previous adsorption period in the dark of 30 min. After a short (2 min) induction period, the disappearance was achieved within less than 8 min.

The initial catalytic quantum yield is defined as the ratio of the number of molecules transformed per second to the number of incident efficient photons (i.e., absorbable by titania) per second.

$$\rho_0 = r_0/\varphi. \qquad [7]$$

The initial rate of disappearance of indigo carmine being equal to 0.90 μmol L^{-1} min^{-1} corresponds to 1.81×10^{14} molecules converted per second. The efficient photonic flux φ, calculated as indicated above, was equal to 5.20×10^{16} photons s^{-1} and the resulting initial quantum yield was found equal to $\rho_0 = r_0/\varphi = 0.35\%$, in good agreement with previous results on other pollutants (12). It has to be mentioned that the kinetics $r = f(C)$ generally follows a Langmuir–Hinshelwood mechanism (12, 22), with a plateau at $C > 5 \times 10^{-3}$ mol L^{-1} and a linear increase at low

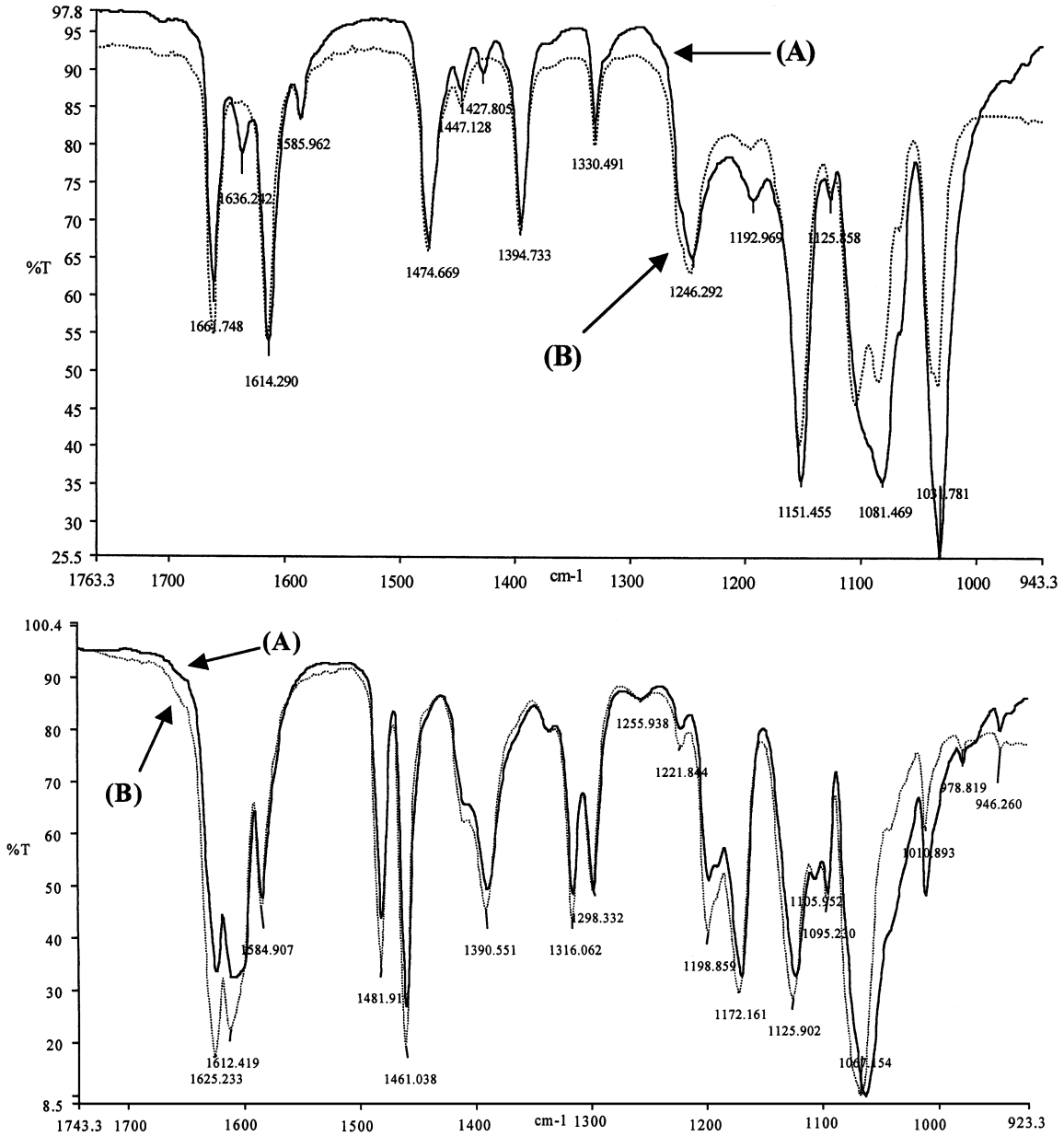

FIG. 4. (Upper figure): Changes of infrared absorption bands of indigo carmine. Curve A: without TiO_2. Curve B: in the presence of TiO_2. (Lower figure): Changes of infrared absorption bands of indigo. Curve A: without TiO_2. curve B: in the presence of TiO_2.

concentrations. This catalytic quantum yield could be consequently higher for higher concentrations, but presently it is high enough to ensure a reasonable degradation of diluted indigo carmine solutions. This confirms the sensitivity of this dye to oxidizing agents (24).

1.3.2. Mineralization. The total degradation leads to the conversion of organic carbon into gaseous CO_2, whereas nitrogen and sulfur heteroatoms are converted into inorganic ions, such as nitrate and ammonium, and sulfate ions, respectively. The formation of CO_2 and of inorganic ions is reported in Fig. 5 for indigo carmine and for indigo. The difference between the observed and the expected quantities of CO_2 is probably due to the persistence of some intermediate products and to the loss of volatile ones. The identification of the main organic intermediate products will be presented further. The quantity of sulfate ions is lower than that expected from stoichiometry, which can be explained by the strong adsorption of SO_4^{2-} at the surface of titania, as previously indicated (25). Figure 5 shows a difference in the initial formation of nitrogen-containing ions between indigo and indigo carmine. This point will be

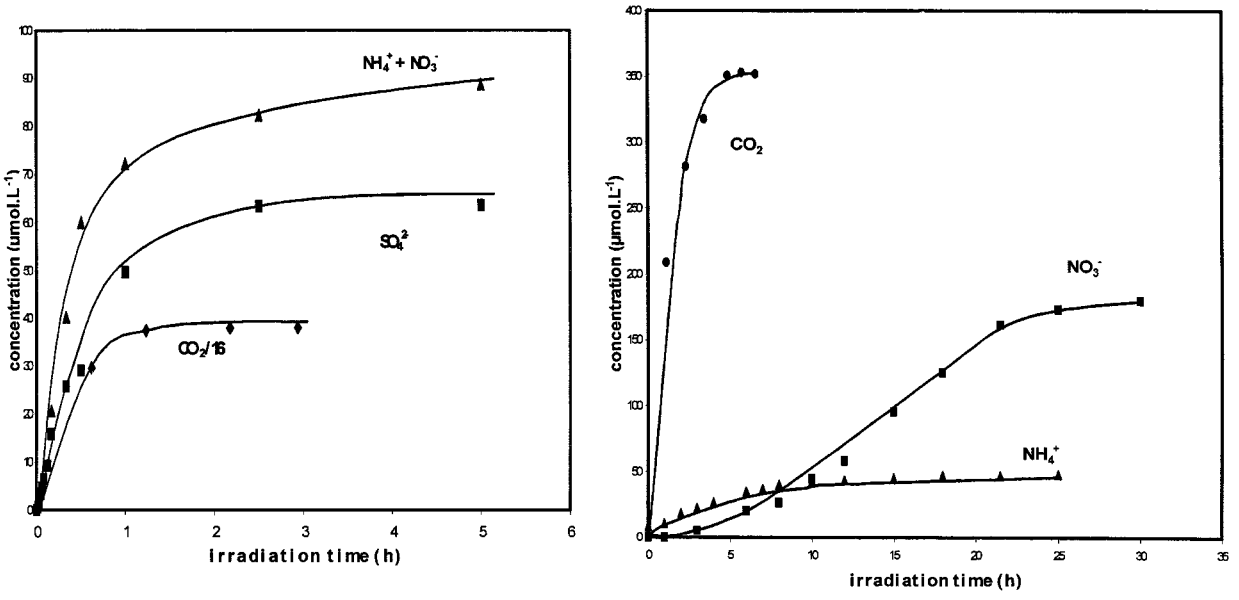

FIG. 5. Evolution of sulfate, nitrate, and ammonium ions in the solution and of gaseous CO_2 during photocatalytic degradation of indigo carmine (A) and of indigo (B).

discussed further. For both dyes, ammonium ions formed are slowly oxidized into nitrate ions, corresponding to the stable maximum oxidation state of nitrogen (+5).

1.3.3. Influence of sulfonate groups. Sulfonate groups in indigo carmine are responsible for the differences between indigo and indigo carmine behaviors. As seen in Section 1.2, the adsorption mode is different for both dyes. From Fig. 5A, SO_4^{2-} ions appear as a primary product since its initial rate ($d[SO_4^{2-}]/dt_0 = 0.6\ \mu mol\ L^{-1}\ min^{-1}$) is close to the overall initial rate r_0 ($r_0 = -d[IC]/dt = 0.9\ \mu mol\ L^{-1}\ min^{-1}$). The difference between both initial rates can be ascribed to a partially irreversible adsorption of SO_4^{2-} ions, already observed for sulfur-containing pesticides but without being detrimental for photocatalysis (25, 26). Therefore, the initial step of IC degradation can be ascribed to the cleavage of the C–S bond, leading to monosulfonated indigo and sulfate ions. The adsorption mode of indigo carmine through its sulfonate groups would favor the attack by photo-generated oxidizing agents, such as h^+ and/or $OH^\bullet$.

At the beginning of degradation, nitrate and ammonium ions are simultaneously formed for indigo carmine ($r_0(NO_3^-) = 0.2\ \mu mol\ L^{-1}\ min^{-1}$, $r_0(NH_4^+) = 1.9\ \mu mol\ L^{-1}\ min^{-1}$), whereas indigo only produces ammonium ions ($r_0(NH_4^+) = 2.8\ \mu mol\ L^{-1}\ min^{-1}$). These results are related to the influence of the sulfonate groups. The electrophilic attack of nitrogen atoms in the dye molecule may be favored by the presence of the sulfonate electro-attractor groups, which weaken the electronic density of the aromatic rings. By contrast, the initial steps of the degradation of the flat molecule of indigo, supposed to adsorb parallel to the surface as mentioned above, do not concern the amino groups, allowing nitrogen atoms to conserve their initial (−3) oxidation state.

1.3.4. Identification of intermediate products. The intermediates generated during the degradation process were analyzed both by HPLC and by GC-MS and identified by comparison with commercial standards and by interpretation of their fragment ions in the mass spectra. It has been attempted to identify (i) the main aromatic metabolites resulting from both indigo and indigo carmine and (ii) especially the carboxylic acid intermediates since their decarboxylation according to the "photo-Kolbe" reaction

$$R\text{–}COO^- + h^+ \rightarrow R^\circ + CO_2 \qquad [6]$$

is the main source of CO_2 evolution all along the various steps of the degradation process. These intermediates are listed in Table 1. The main aromatic metabolites for indigo were 2-nitrobenzaldehyde and anthranilic (2-aminobenzoic) acid. This clearly indicates that indigo initially reacts at the level of the central double bond, in agreement with an adsorption parallel to the surface as indicated in Section 1.2.

Nitrobenzene could only be detected in IC degradation. This could be related to the initial degradation step of IC involving the attack of the aromatic ring by abstraction of the sulfonic substituent linked to the surface of titania. The subsequent photocatalytic degradation of these aromatic intermediates has been well known since our previous studies (for instance, Ref. (27) for nitrobenzene and Ref. (28) for substituted benzoic acids).

The identification of aliphatic fragments, mainly carboxylic acids (Table 1), is particularly instructive. Considering

TABLE 1

Main Intermediate Products Detected during Photocatalytic Degradation of Indigo Carmine and of Indigo

Compounds	Analytical techniques	Retention time (min)	Molecular weight (g/mol)
2-Nitro-benzaldehyde and/or 2,3-dihydroxy-indoline	GC-MS		151
Anthranilic acid	HPLC-UV GC-MS	21.8	137
Tartaric acid	HPLC-UV GC-MS	7.9	150
Malic acid	HPLC-UV GC-MS	8.9	134
Amino-fumaric acid	GC-MS		131
Pyruvic acid	HPLC-UV GC-MS	8.4	88
Malonaldehydic acid	HPLC-UV	9.3	
Malonic acid	HPLC-UV GC-MS	9.3	104
3-Amino propenoic acid	GC-MS		87
Glycolic acid	HPLC-UV GC-MS	11.3	76
Oxalic acid	HPLC-UV GC-MS	6.4	90
Acrylic acid	HPLC-UV	17.9	59
3-Amino; 2,3-dihydroxy-propanoic acid	GC-MS		121
Acetic acid	HPLC-UV	13.8	60

the developed formulae, it can be conceived that the formation of nitrobenzene produces unsaturated trans-C_4 fumaric acid, which by oxidation, generates malic and tartaric acids. In parallel, the formation of anthranilic acid can be associated with that of C_3-carboxylic (acrylic, tartronic, and pyruvic) acids.

The central C=C double bond has been found very reactive since the previous study of gas phase photo-oxidation of propene producing an epoxide as a primary product (29). Presently, the initial step of the reaction could be the C=C double-bond cleavage, thus explaining the initial evolution of CO_2 ($d[CO_2]/dt > 0$ at $t_{UV} = 0$) resulting from anthranilic acid formation followed by its decarboxylation.

The part of intermediates originating from the nondissociation of the central C=C double bond concerns fumaric and 2,3-dihydroxyfumaric acids as well as two amino products: 3-amino-glyceric acid and 1,2-diaminoglycol. The photocatalytic degradation of malic acid and of its metabolites has previously been accurately studied as a polycarboxylic compound found in the biomass and in degradation products of complex molecules (30). Its present identification in indigo degradation products enables us to account for the C_2–C_4 carboxylic metabolites observed.

The kinetics of formation of intermediate acids during the degradation of indigo carmine and of indigo are represented in Fig. 6. The first acids formed after 20 min of UV irradiation are oxalic, anthranilic, and malic acids, in line with the complete bleaching of the dye in 8 min. The shorter carboxylic acids appear subsequently, with a maximum amount obtained after ca. 30 min of UV irradiation. All the intermediate products, except acetic acid, are degraded within 1 h of UV irradiation, in agreement with the time of formation of CO_2 (1 h). Acetic acid requires a longer time for mineralization, as generally observed. A tentative mechanism of degradation inferred from these data is reported in Scheme 2.

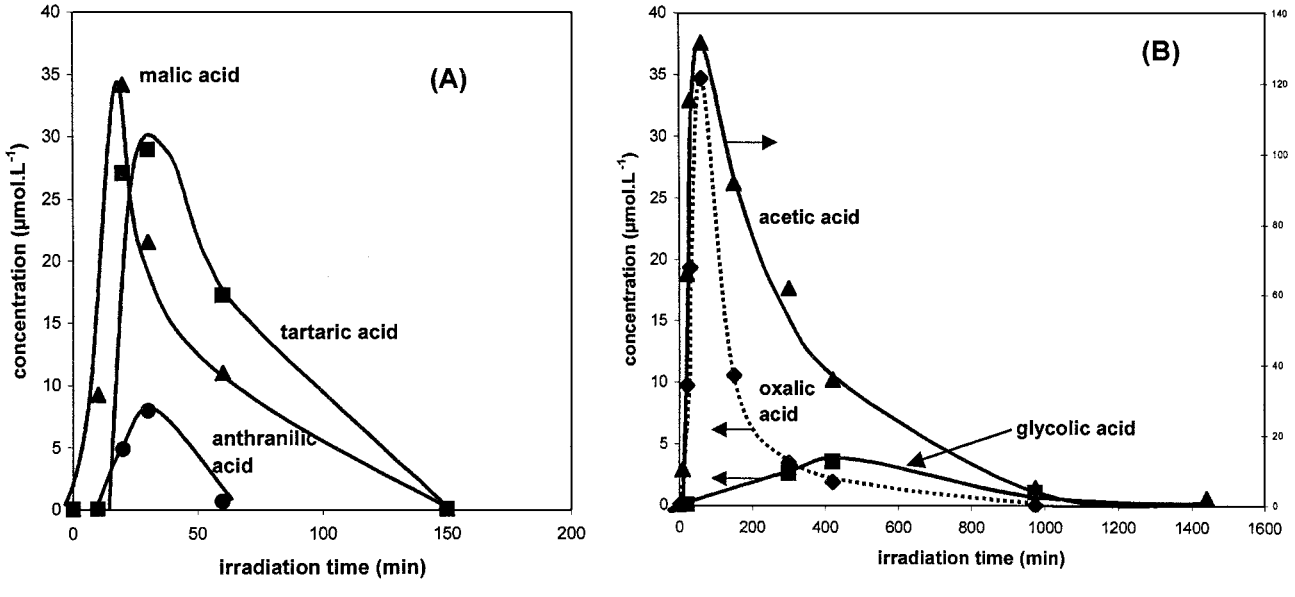

FIG. 6. Evolution of the main intermediate acids detected during the photocatalytic degradation of indigo carmine and of indigo. (A) C_n acids ($n \geq 4$); (B) C_2 acids.

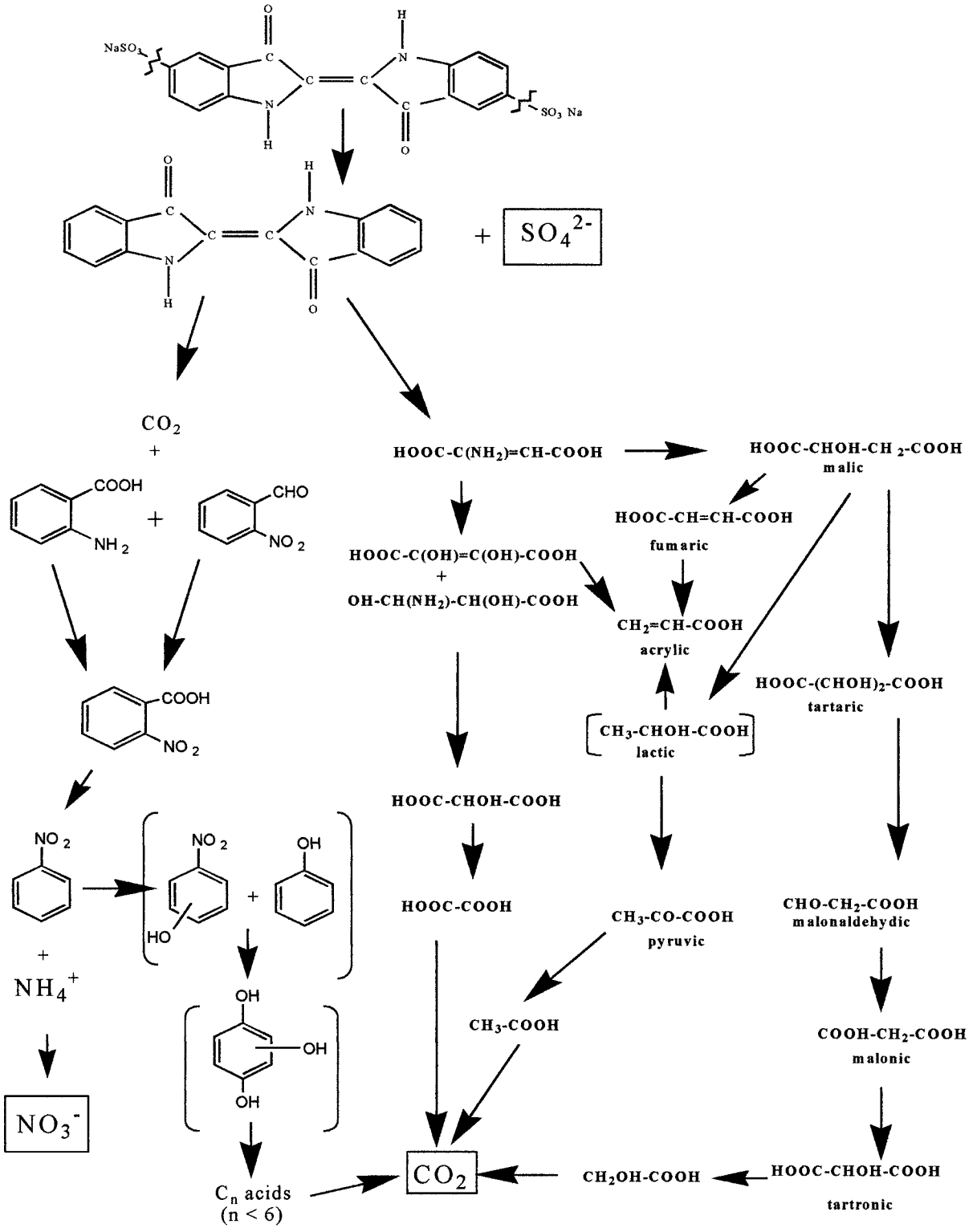

SCHEME 2. Mechanism of the photocatalytic degradation of indigo carmine and of indigo.

The different metabolites duly identified are logically reported according to their decreasing molecular weight. Photocatalytic oxidation in water is not selective by contrast with selective mild oxidation in a pure gaseous or liquid phase of aliphatic or substituted aromatic hydrocarbons as discussed in Ref. (12). Two oxidative agents can be considered: the photo-produced holes h^+ and/or OH° radicals, which are known as strongly active and degrading but nonselective agents. Holes are mainly involved in the decarboxylation reaction ("photo-Kolbe") (Eq. [6]). OH° radicals can be generated by various reactions:

—(i) oxidation of water by holes

$$(H_2O \Leftrightarrow H^+ + OH^-) + h^+ \rightarrow H^+ + OH^\circ; \qquad [8]$$

—(ii) transient formation of hydroperoxide radicals

$$O_2(g) + e^- \rightarrow O_2^{\circ -} \qquad [9]$$

$$O_2^{\circ -} + H^+ \rightarrow HO_2^\circ \qquad [10]$$

$$2HO_2^\circ \rightarrow H_2O_2 + O_2 \qquad [11]$$

$$H_2O_2 + e^- \rightarrow OH^- + OH^\circ. \qquad [12]$$

In the present case, the OH° radicals can break the various C–N and C–C bonds of the chromophore group as described in Scheme 2, thus accounting for the various metabolites identified.

The aromatic intermediates found (anthranilic acid, nitrobenzaldehyde, nitrobenzoic acid, and nitrobenzene) undergo successive attacks by OH° radicals, giving hydroxylations and/or substitutions generally leading to hydroxyhydroquinone known as the last aromatic molecule found before the aromatic ring opening. Presently, no C_5 to C_{10} aliphatic acids were detected, corresponding to fragments consecutive with the ring opening. Either they were in minute undetectable amounts or they remained mainly at the surface or in the double layer without transient desorption in water.

2. Decolorization of Indigo Carmine in an Aqueous Suspension of TiO_2 Irradiated by Visible Light

Irradiation by visible light induces changes in the decolorization mechanism. Although TiO_2 cannot be directly activated by visible irradiation with an energy <3.1 eV (band gap energy of anatase), visible light can induce the excitation of the dye molecule. Previous works have reported the electron injection from excited dye molecules into polycrystalline TiO_2 electrodes (30). Electron transfer from adsorbed dye molecules to surface-acceptor sites was proved to be effective for molecules in the excited state since (i) the energy level of the donor orbital of the excited dye molecule is sufficiently high above the conduction band edge of the oxide and (ii) the density of acceptor sites often increases toward the edge of the conduction band (31, 32). Such a transfer has already been observed for cresyl violet (32).

2.1. Kinetics of Decolorization

The kinetics of bleaching is represented in Fig. 7. The total decolorization of indigo carmine by visible-irradiated

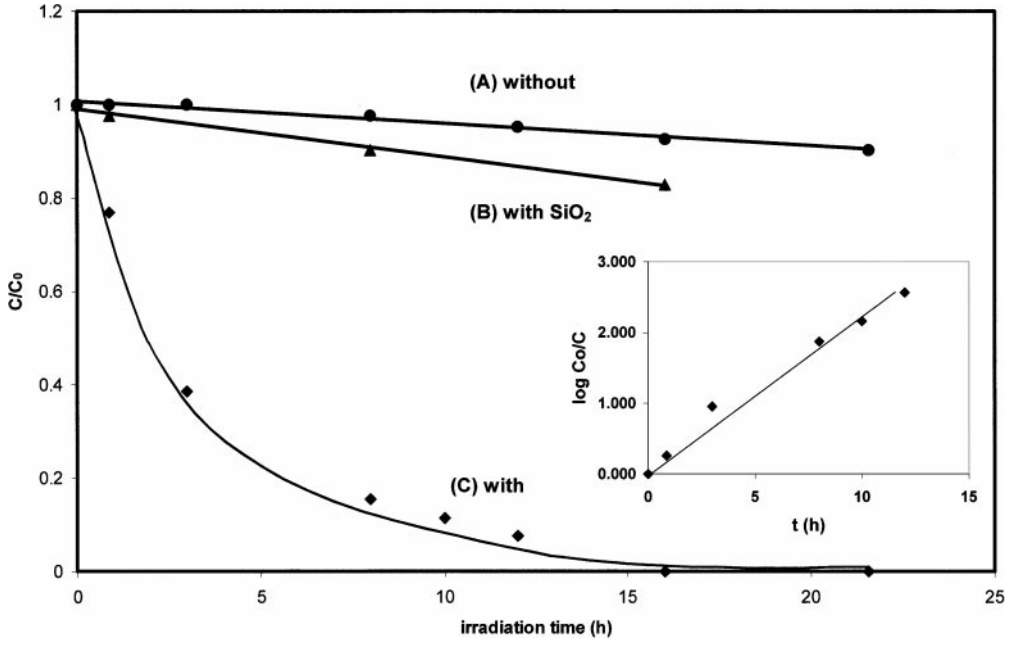

FIG. 7. Kinetics of decolorization (bleaching) of indigo carmine using visible light. Curve A: without any solid. Curve B: with photo-inactive SiO_2. Curve C: with TiO_2 photocatalyst.

titania was reached within 16 h, following a first-order kinetics ($k = 8 \times 10^{-3}$ min^{-1}). A solution without titania and a blank suspension of photo-inert SiO_2 were irradiated for 16 h in the same conditions (see Fig. 7). The decrease in concentration was equal to 7 and 17%, respectively. From the two blank tests, it was inferred that visible-light-induced decolorization necessarily involves titania. However, titania being quite photo-inactive at $\lambda > 440$ nm, the process of the photo-bleaching has to involve the dye as a sensitizer.

2.2. Nature of the Reaction

No intermediates and no final mineralization products were found in the solution, indicating that the dye is only decolorized but not degraded. This was confirmed by TOC analyses, which revealed not only that no degradation occurred but also that there remained the same quantity of IC adsorbed after visible irradiation (0.15 molecule/nm^2 as before irradiation at the end of the adsorption period in the dark (0.13 molecule/nm^2). Scheme 3 represents an energy diagram under UV and visible irradiation. Under UV, titania gets excited and indigo carmine can cede an electron to its valence band either directly or indirectly via an attack by OH° radicals. Under visible light, only indigo carmine becomes excited at $\lambda > 440$ nm with the promotion of an electron in an upper orbital, whose relative energy level enables the transfer of one electron into the conduction band of the catalyst. This transfer could be favored by a driving force consisting of a subsequent electron transfer to an adsorbed oxygen molecule. The present photo-bleaching of indigo carmine only corresponds to decolorization by loss of conjugation of the double bonds in the whole molecule induced by the electron transfer to titania. In titania-based photocatalysis, the actual oxidizing species at the origin is the photo-produced hole h^+. The subsequent oxidizing and degradation chemical agent is the OH° radical mostly formed by oxidation of water (Eq. [8]). Presently, the absence of holes (see Scheme 3B) implies the absence of OH° radicals and subsequently of any degradation, as observed for quinones (34). Since no subsequent degradation occurs, this means that this electron transfer should be stoichiometric. This has been checked by using an initial number of indigo carmine molecules 2.5 times higher than the maximum number of O_2^- sites deduced from a saturation coverage of 5×10^{18}/m^2 (23): the discolorization did not occur even after 36 h of continuous visible illumination.

Eventually, it has to be mentioned that our results are in contrast to the degradation obtained in the visible with alizarin red (17) and with acid orange 7 (33).

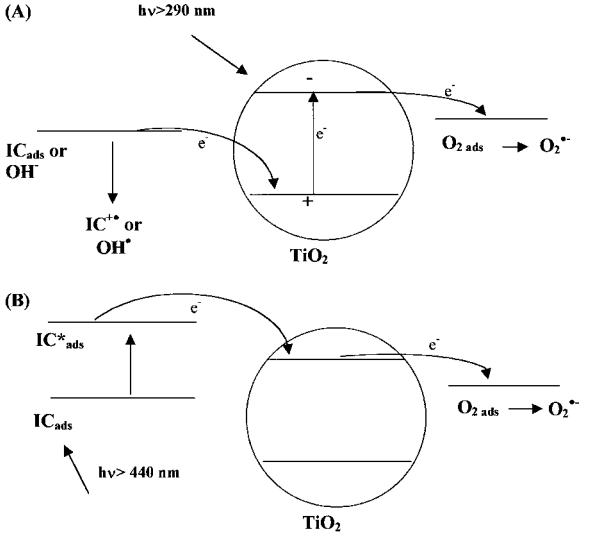

SCHEME 3. Mechanism of TiO_2-assisted photodecolorization (A) under UV irradiation and (B) under visible light.

3. Photocatalytic Degradation of Solid Indigo

The poor solubility of indigo prompted us to assess a possible photocatalytic reaction in a biphasic solid–solid system. The possible lack of water in the photocatalytic degradation of solid indigo preventing the formation of OH° radicals (Eqs. [8]–[12]) has been taken into consideration. Actually, the preparation of the layer constituted by a mixture of titania and of solid indigo consisted merely of evaporation at room temperature of a slurry deposited on the optical disk support. This enabled full coverage of titania in water at $t_{UV} = 0$. In addition, photodegradation produces water, which maintains a sufficient hygroscopic level at the surface and (ii) ambient air moisture always keeps titania's surface (which is highly hydrophilic) in an hydrated state.

The results obtained on optical disks (Fig. 8) clearly indicated a photobleaching of solid indigo mechanically mixed with powder titania.

3.1. Kinetics of Disappearance

The disappearance of solid indigo is reported in Fig. 9. It follows an apparent first-order kinetics ($k = 9 \times 10^{-3}$ min^{-1}). The final level is reached within 9 h. This much longer period of time compared with that of the disappearance of indigo carmine in water has to be attributed to the slow diffusion of the oxidizing agents (h^+, OH°) on the surface of the photocatalyst, diffusion becoming the rate-limiting step of the whole process.

3.2. Mineralization

The formation of CO_2 was chosen as experimental proof for degradation. The maximum amount of CO_2 formed was achieved in 20 h and corresponded to a conversion of 33%, as shown in Fig. 9. Three reasons may explain this result: (i) the loss of volatile species formed during the

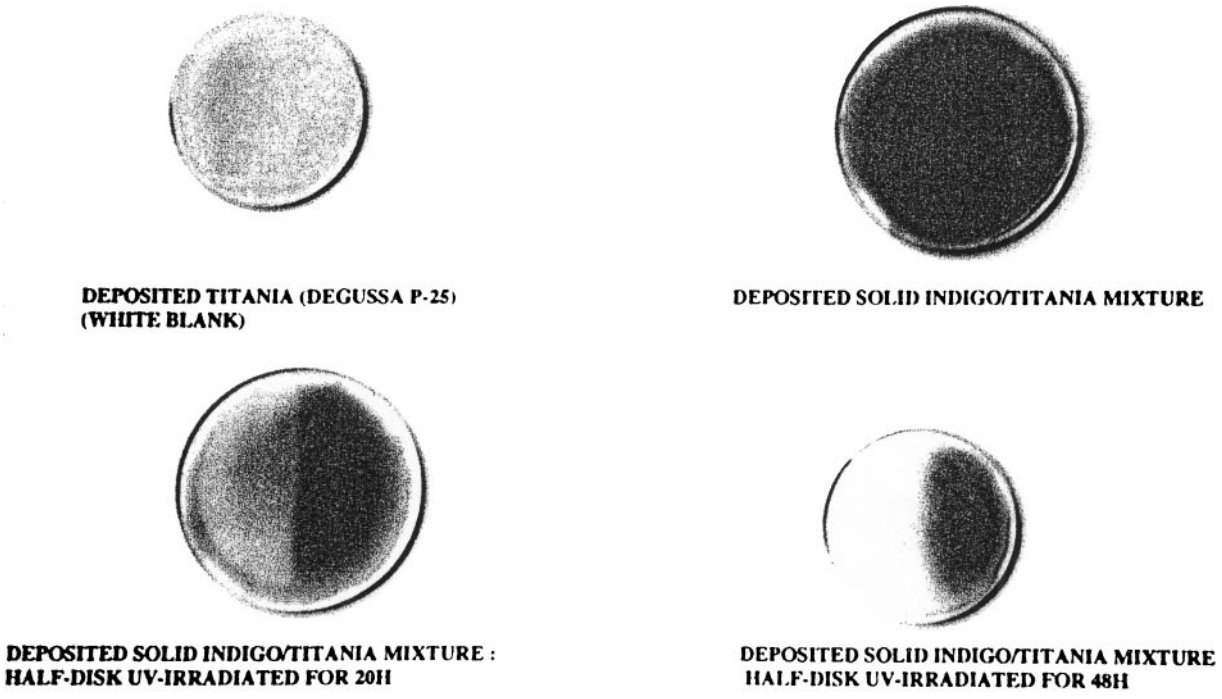

FIG. 8. Decolorization of solid indigo.

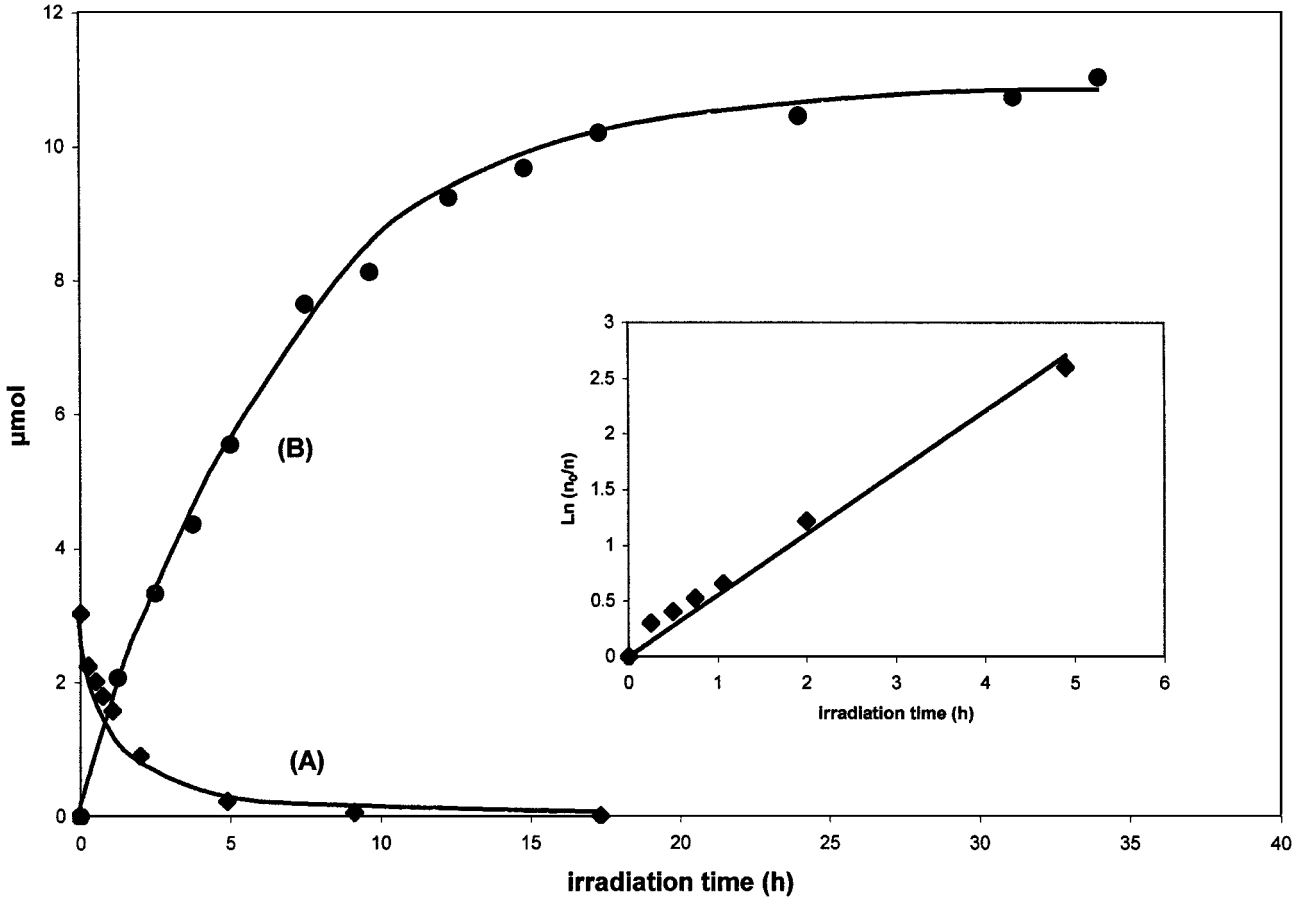

FIG. 9. Kinetics of the photocatalytic degradation of solid indigo. Curve A: disappearance of indigo. Curve B: evolution of CO_2 formed during UV irradiation. Insert: semi-log linear transform of curve A.

TABLE 2

Main Intermediate Products Detected during Photocatalytic Degradation of Solid Indigo

Compounds	Analytical techniques	Retention time (min)	Molecular weight (g/mol)
2-Nitrobenzoic acid	GC-MS		167
Nitrobenzene	GC-MS		123
Malic acid	HPLC-UV	8.8	134
	GC-MS		
Fumaric acid	HPLC-UV	15.8	116
	GC-MS		
Dihydroxyfumaric acid	GC-MS		148
Glycolic acid	HPLC-UV		
	GC-MS	11.5	76
Oxalic acid	HPLC-UV		
	GC-MS	6.4	90
Acetic acid	HPLC-UV	13.8	60

degradation, (ii) the persistence of non-photodegraded by-products, and (iii) the heterogeneity of the deposit, which prevents some solid indigo particles from being directly in contact with titania crystallites.

3.3. Identification of Intermediate Products

The same procedures and analytical techniques as those in Section 1.3.4. were used to identify the intermediate products. The main molecules detected are presented in Table 2. They are similar to those obtained in water suspensions so that the same degradation mechanism can be proposed. Two additional nitro compounds (Table 2) were identified by GC/MS, suggesting a transient accumulation of these products in the absence of water, thus favoring their detection. They have been included in the general degradation pathway in Scheme 2.

The photocatalytic degradation of solid indigo, mechanically mixed with powder titania and placed in a fixed catalytic bed, constitutes one of the first examples (or maybe the first one) of a photocatalytic reaction using a solid reactant. The only—and undesirable—known example is the photo-(solar-)degradation of plastics or paints, pigmented with deficiently passivated titania. Natural weathering gradually produces a "chalking effect," which is caused by the progressive elimination of the organic polymeric binder and via a (slow) photocatalytic combustion of the organic matter in contact with an ill-protected titania-based opacifier (18, 35).

The positive decolorization and degradation of solid indigo, illustrated by Fig. 8, constitutes an encouraging result for the use of outdoor self-cleaning titania-coated surfaces such as glasses (36–38), stainless steel (37), walls, etc.) fouled by solid dirt particles.

CONCLUSIONS

The photocatalytic degradation of indigo and of indigo carmine has been successfully demonstrated when using UV-irradiated titania-based catalysts. In addition to a prompt removal of the color, photocatalysis was simultaneously able to oxidize the dye, with an almost complete mineralization of carbon and of nitrogen and sulfur heteroatoms into innocuous compounds. A detailed degradation pathway, based on careful identification of intermediate products, is proposed.

The irradiation of titania in the visible light produces a photoinduced decolorization of the dye but without any degradation, corresponding to a stoichiometric electron transfer from the dye, excited in the visible irradiation, to titania. The positive decolorization and degradation of solid indigo, mechanically mixed, constitutes an encouraging result for self-cleaning titania-coated objects (glasses, steel, walls, etc.) fouled by solid dirt particles.

The ensemble of these results clearly suggest that TiO_2/UV photocatalysis may be envisaged as a method for treatment of diluted colored waste waters in textile industries, especially in sunny semi-arid countries where water has to be recycled. Large solar pilot experiments are programmed for this purpose.

ACKNOWLEDGMENTS

This work was supported by a CMCU Project (99F1201). The authors are grateful to Michelle Besson and Marie-Laure Moulut for the TOC analyses.

REFERENCES

1. "Color Chemistry. Synthesis, Properties and Applications of Organic Dyes and Pigments" (H. Zollinger, Ed.), 2nd revised ed. VCH, New York, 1991.
2. Dejohn, P. B., and Hutchins, R. A., *Tex. Chem. Color.* **8**, 69 (1976).
3. Patil, S. S., and Shinde, V. M., *Environ. Sci. Technol.* **22**, 1160 (1988).
4. More, A. T., Vira, A., and Fogel, S., *Environ. Sci. Technol.* **23**, 403 (1989).
5. Slokar, Y. M., and Le Marechal, A. M., *Dyes Pigments* **37**, 335 (1998).
6. "Photocatalysis and Environment. Trends and Applications" (M. Schiavello, Ed.), Kluwer, Dordrecht, 1988.
7. "Photocatalysis. Fundamentals and Applications" (N. Serpone, and E. Pelizzetti, Eds.), Wiley Interscience, New York, 1989.
8. Guillard, C., Herrmann, J. M., and Pichat, P., *Catal. Today* **17**, 7 (1993).
9. "Photocatalytic Purification and Treatment of Water and Air" (H. A. Al-Ekabi, and D. Ollis, Eds.), Elsevier, Amsterdam, 1993.
10. Bahnemann, D. W., Cunningham, J., Fox, M. A., Pelizzetti, E., Pichat, P., and Serpone, N., *in* "Aquatic Surface Photochemistry" (R. G. Zeep, G. R. Helz, and D. G. Crosby, Eds.), p. 261. F.L. Lewis, Boca Raton, FL, 1994.
11. Legrini, O., Oliveros, E., and Braun, A. M., *Chem. Rev.* **93**, 671 (1993).
12. Herrmann, J. M., chapter 9 *in* "Environmental Catalysis" (F. Jansen and R. A. van Santen, Eds.), Catalytic Science Series, pp. 171–194. Imperial College Press, London, 1999.
13. Blake, D. M., "Bibliography of Work on the Photocatalytic Removal of Hazardous Compounds from Water and air," NREL/TP-430-22197. National Renewable Energy Laboratory, Golden, CO, 1997 and 1999.

14. Pulgarin, C., Pajonk, G. M., Bandara, J., and Kiwi, J., "Meeting ACS Division of Environmental Chemistry, Anaheim, CA, 1995," Paper No. 232, p. 767. Am. Chem. Soc., Washington, DC, 1995.
15. Zhang, F., Zhao, J., Shen, T., Hidaka, H., Pelizzetti, E., and Serpone, N., *Appl. Catal. B* **15**, 147 (1998).
16. Wu, G., Wu, T., Zhao, J., Hidaka, H., and Serpone, N., *Environ. Sci. Technol.* **33**, 2081 (1999).
17. Liu, G., Li, X., Zhao, J., Horikoshi, S., and Hidaka, H., *J. Mol. Catal. A* **153**, 221 (2000).
18. Kämpf, G., and Völz, H. G., *Farbe Lack* **74**, 37 (1968).
19. "The Sigma Aldrich Handbook of Stains, Dyes and Indicators" (F. J. Green, Ed.), pp. 403–406. Aldrich Chemical, Milwaukee, WI, 1990.
20. Rademacher, P., and Kowski, K., *Chem. Ber.* **125**, 1773 (1992).
21. Yang, Y., Wyatt, D. T., and Bahorsky, M., *Textile Chem. Color.* **30**, 27 (1998).
22. Herrmann, J. M., *Catal. Today* **24**, 157 (1995).
23. Boehm, H. P., *Adv. Catal.* **16**, 179 (1966).
24. Roberts, E. L., Burguieres, S., and Warner, I. M., *Appl. Spectrosc.* **52**, 1305 (1998).
25. Herrmann, J. M., Guillard, C., Arguello, M., Agüera, A., Tejedor, A., Piedra, L., and Fernandez-Alba, A., *Catal. Today* **54**, 353 (1999).
26. Kerzhentsev, M., Guillard, C., Herrmann, J.-M., and Pichat, P., *Catal. Today* **27**, 215 (1996).
27. Maillard-Dupuis, C., Guillard, C., and Pichat, P., *New J. Chem.* **18**, 941 (1994).
28. Herrmann, J. M., Tahiri, H., Guillard, C., and Pichat, P., *Catal. Today* **54**, 131 (1999).
29. Pichat, P., Herrmann, J. M., Disdier, J., and Mozzanega, M. N., *J. Phys. Chem.* **83**, 3122 (1979).
30. Vlachopoulos, N., Liska, P., Augustynski, J., and Grätzel, M., *J. Am. Chem. Soc.* **110**, 1216 (1988).
31. Spitler, M., and Calvin, M., *J. Chem. Phys.* **66**, 4294 (1976).
32. Kietzmann, R., Willig, F., Weller, H., Vogel, R., Nath, D. N., Eichberger, R., Liska, P., and Lehnert, J., *Mol. Cryst. Liq. Cryst.* **194**, 169 (1991).
33. Vinogdopal, K., Wynkoop, D. E., and Kamat, P. V., *Environ. Sci. Technol.* **30**, 1660 (1996).
34. Nasr, C., Vinogdopal, K., Ficher, L., Hotchandani, S., Cattopadhyay, A. K., and Kamat, P. V., *J. Phys. Chem.* **100**, 8436 (1996).
35. Kaempf, G., *J. Coating Technol.* **51**, 51 (1979).
36. Fujishima, A., *Look Jpn.* **41**, 47 (1995).
37. Fernandez, A., Lassaletta, G., Jimenez, V. M., Justo, A., Gonzalez-Elipe, A. R., Herrmann J. M., Tahiri, H., and Ait-Ichou, Y., *Appl. Catal. B* **7**, 49 (1995).
38. Heller, A., *Acc. Chem. Res.* **28**, 503 (1995).
39. Romeas, V., Pichat, P., Guillard, C., Chopin, T., and Lehaut, C., *New J. Chem.* **23**, 365 (1999).